Eur. Phys. J. C (2023) 83:959
https://doi.org/10.1140/epjc/s10052-023-12105-6

THE EUROPEAN PHYSICAL JOURNAL C

Regular Article - Theoretical Physics

Viscous QCD medium effects on the bottom quark transport coefficients

Adiba Shaikh[a], **Sadhana Dash**[b], **Basanta K. Nandi**[c]

Department of Physics, Indian Institute of Technology Bombay, Powai, Mumbai 400076, India

Received: 26 February 2023 / Accepted: 4 October 2023 / Published online: 24 October 2023

Abstract The bottom quark transport coefficients, i.e., drag and diffusion coefficients, have been studied for the collisional and soft gluon radiative processes within the viscous QCD medium. The thermal medium effects are incorporated using the effective fugacity quasiparticle model (EQPM). Both the shear and bulk viscous effects at leading order are embedded through the near-equilibrium distribution functions of the quark–gluon plasma (QGP) constituent quasiparticles. The transport coefficients' dependence on the bottom quark's initial momentum and QGP temperature have been investigated. The relative dominance of the radiative over the collisional process for the bottom quark seems to occur at a higher initial momentum compared to that of the charm quark. In contrast, the effect of the viscous corrections seems to be more for the charm quark. Furthermore, we also investigate the validity of the Einstein fluctuation–dissipation theorem for our analysis.

1 Introduction

Hadrons, under extreme conditions like high temperatures ($T \gtrsim 200$ MeV $\approx 10^{12}\,K$) and/or high baryonic densities ($\mu \gtrsim 200$ MeV) undergo phase transition into the deconfined state of quarks, anti-quarks and gluons as the effective degrees of freedom. Such conditions which are believed to exist only in the early universe and inside the core of the neutron star are recreated in the experiments at some of the largest particle accelerators like the Relativistic Heavy Ion Collider (RHIC) and Large Hadron Collider (LHC) in a controlled environment to investigate its properties [6,8,13,14]. Relativistic viscous hydrodynamics have successfully described the evolution of the QGP phase involving various dissipative processes [33,41,44]. The transport coefficients which are sensitive to medium evolution are theoretically calculated by the underlying microscopic theory like the effective kinetic theory approach [1,42] and compared with those extracted experimentally. Within dissipative hydrodynamics, the effect and evolution of the QGP medium through the spatial anisotropy and pressure gradients are explored by introducing the shear and bulk viscosity respectively [58,59].

Heavy quarks like charm and bottom are created in the early stages of the heavy-ion collision, primarily due to partonic hard scattering such as the gluon fusion process. Such heavy quarks within the medium introduce an energy scale, i.e., their mass (m_{HQ}) which is an order of magnitude larger than the temperature of the QGP medium ($T \approx 500$ MeV). Due to their large mass ($m_c \approx 1.3$ GeV, $m_b \approx 4.2$ GeV), they do not thermalize with the plasma over its lifetime and traverse through the plasma unequilibrated. Hence, they act as an excellent probe to study QGP evolution and its properties [2,12,16,32,57]. Also, heavy quarks, being heavier than the typical strong interaction confinement scale $\Lambda_{QCD} \approx 200$ MeV, can be treated non-relativistically having a small strong coupling constant ($\alpha_s \approx 0.1 - 0.3$) in the realm of perturbative QCD. Heavy quarks undergo energy loss while traversing through QGP due to collision ($2 \to 2$, elastic) with the plasma constituents and radiation of the soft gluons ($2 \to 3$, inelastic). Collisional energy loss is dominant for the heavy quark with low momentum whereas at high momentum medium induced gluon radiation becomes dominant [3,19,22–24,27,36,51,53,56,60,70,75].

The movement of heavy quarks within QCD plasma can be treated as a Brownian motion of massive particles within the fluid. Hence, the phase space evolution of the heavy quarks is governed by the Boltzmann transport equation. Further, the soft-scattering approximation of momentum transfer between heavy quarks and in-medium

[a] e-mail: adibashaikh9@gmail.com (corresponding author)
[b] e-mail: sadhana@phy.iitb.ac.in
[c] e-mail: basanta@phy.iitb.ac.in

particles reduces the transport equation to the Fokker–Planck equation, where its interaction with the medium constituents (quarks, anti-quarks and gluons) is incorporated through the drag and momentum diffusion coefficients [28,34,69]. Heavy quark transport coefficients are sensitive to the medium evolution in the presence of dissipative processes within QGP. The transport coefficients associated with the dissipative processes (viscosity, electric conductivity, etc.) in the hot and dense QCD medium can be determined from the underlying microscopic theories, such as the effective kinetic theory approach. They could also be extracted experimentally at RHIC and LHC through various observables and phenomenological transport models and, using lattice QCD [5,7,9–11,15,20,21,30,31,35,38–40,45,50,61,67,71,73,74]. The viscous corrections to the heavy quark transport coefficients for the collisional processes have been previously studied [29,48,49,64,66]. Here, we go a step further to investigate the effect of viscous corrections on the radiative process of the bottom quarks as a follow-up to our previous study for the charm quark [62].

In this work, we study the impact of the shear and bulk viscosities of the QGP on the drag and diffusion coefficients of the bottom quark for collision and radiative processes. The thermal QCD medium interactions with the realistic equation of state effects are incorporated using the effective fugacity quasiparticle model (EQPM) [25,26]. This model considers QGP as a medium of non-interacting quasiparticles with dynamical effects included in the dispersion relation of constituent particles through the introduction of the effective fugacity parameter. For viscous corrections, the non-equilibrium distribution function has been obtained by solving the effective Boltzmann equation based on the EQPM with the relaxation time approximation (RTA) and using the Chapman-Enskog like iterative expansion method [54]. The collective mean-field contributions originating from the underlying conservation laws are included in the determination of the near-equilibrium momentum distribution functions. Here, we present the result for the effect of shear and bulk viscous corrections on the radiative process of the bottom quark in terms of its transport coefficients and compare it to the collisional process. We observe a considerable modification in the drag and diffusion coefficients of the bottom quark due to these corrections, compared to the charm quark previously studied in [63]. The bottom quark is roughly three times heavier than the charm quark with a large thermal relaxation time and intrinsic mass scale being very far from the non-perturbative QCD confinement scale ($\Lambda_{QCD} \approx 200$ MeV). Therefore, it is a better probe for the investigation of the in-medium properties via its transport coefficients and motivation for the present work.

In Sect. 2, the formulation of the heavy quark dynamics in the QCD medium is discussed for collisional and radiative processes followed by the EQPM description of viscous corrections to the momentum distribution function of the quasiparticles. Section 3 focuses on the results for the transport coefficients of the bottom quark including shear and bulk viscous corrections followed by the comparative study of the energy loss of charm and bottom. We summarize with the conclusion in Sect. 4.

Notations and conventions: The subscript k denotes the particle species, where $k = lq$ represents light quarks, $k = l\bar{q}$ represents light anti-quarks and $k = g$ representing the gluons. The degeneracy factor for gluon is $\gamma_g = N_s \times (N_c^2 - 1)$ and for light quark (antiquark) is $\gamma_{lq} = N_s \times N_c \times N_f$ with $N_s = 2$, $N_f = 3$ (u, d, s), and $N_c = 3$ (for $SU(3)$). u^μ is the normalized fluid velocity satisfying the relation $u^\mu u_\mu = 1$ with the metric tensor $g^{\mu\nu} = \text{diag}(1, -1, -1, -1)$.

2 Formalism

2.1 Heavy quark transport coefficients

We can treat the bottom quark as a Brownian particle (non-equilibrated) moving within the QGP medium (equilibrated) where the massive quark loses its energy due to collision with the medium constituents (elastic process) and also through gluon radiation (inelastic). Both these interactions of the bottom quarks within the QGP medium are incorporated in their transport coefficients.

2.1.1 Collisional (2→2) process

The bottom quark (HQ) undergoes collisions with the medium constituents, *i.e.*, light quarks (lq), light antiquarks ($l\bar{q}$) and gluons (g). The elastic ($2 \to 2$) process is,

$$HQ\ (p) + lq/l\bar{q}/g\ (q) \to HQ\ (p') + lq/l\bar{q}/g\ (q'). \quad (1)$$

The evolution of the bottom quark momentum distribution function f_{HQ} is determined by the Boltzmann transport equation, which within the soft scattering approximation reduces to the Fokker–Planck equation [69],

$$\frac{\partial f_{HQ}}{\partial t} = \frac{\partial}{\partial p_i}\left[A_i(\mathbf{p}) f_{HQ} + \frac{\partial}{\partial p_j}\Big(B_{ij}(\mathbf{p}) f_{HQ}\Big)\right]. \quad (2)$$

$A_i(\mathbf{p})$ is the drag force and $B_{ij}(\mathbf{p})$ is the momentum diffusion tensor for the bottom quark expressed in the form of thermal average as,

$$A_i(\mathbf{p}) = \frac{1}{2E_p\gamma_{HQ}}\int\frac{d^3\mathbf{q}}{(2\pi)^3E_q}\int\frac{d^3\mathbf{q}'}{(2\pi)^3E_{q'}}\int\frac{d^3\mathbf{p}'}{(2\pi)^3E_{p'}} \times\sum|\mathcal{M}_{2\to2}|^2\,(2\pi)^4\,\delta^{(4)}(p+q-p'-q') \times f_k(E_q)\,(1\pm f_k(E_{q'}))\,[(p-p')_i] = \langle\langle(p-p')_i\rangle\rangle, \tag{3}$$

$$B_{ij}(\mathbf{p}) = \frac{1}{2E_p\gamma_{HQ}}\int\frac{d^3\mathbf{q}}{(2\pi)^3E_q}\int\frac{d^3\mathbf{q}'}{(2\pi)^3E_{q'}}\int\frac{d^3\mathbf{p}'}{(2\pi)^3E_{p'}} \times\sum|\mathcal{M}_{2\to2}|^2\,(2\pi)^4\,\delta^{(4)}(p+q-p'-q') \times f_k(E_q)\,(1\pm f_k(E_{q'}))\,[(p-p')_i\,(p-p')_j] = \frac{1}{2}\langle\langle(p-p')_i\,(p-p')_j\rangle\rangle, \tag{4}$$

where $\gamma_{HQ} = N_s \times N_c$ is the heavy quark degeneracy factor. $|\mathcal{M}_{2\to2}|$ represents the scattering amplitude for $2 \to 2$ process (refer Appendix **A** of [63]) and $p = |\mathbf{p}|$ is the magnitude of heavy quark initial momentum. $f_k(E_q)$ denotes the distribution function for quarks, antiquarks ($k = lq, l\bar{q}$) and gluons ($k = g$). For the final state phase space, we have the Fermi suppression factor $(1 - f_{lq}(E_{q'}))$ for light quarks and Bose enhancement factor $(1 + f_g(E_{q'}))$ for gluons. Here, the drag force gives the thermal average of the momentum transfer between the initial and final states of the bottom quark, whereas B_{ij} denotes the square of the momentum transfer as the bottom quark diffuses through the medium. Since, both $A_i(\mathbf{p})$ and $B_{ij}(\mathbf{p})$ depend explicitly on the initial heavy quark momentum ($\mathbf{p}$), the drag coefficient (A) is defined as,

$$A_i = p_i\,A(p^2) \implies A(p^2) = \langle\langle 1\rangle\rangle - \frac{\langle\langle\mathbf{p}.\mathbf{p}'\rangle\rangle}{p^2}. \tag{5}$$

The diffusion tensor decomposed into its transverse and longitudinal components give,

$$B_{ij} = \left[\delta_{ij} - \frac{p_i\,p_j}{p^2}\right]B_0(p^2) + \frac{p_i\,p_j}{p^2}B_1(p^2), \tag{6}$$

where, the transverse momentum diffusion (B_0) and longitudinal momentum diffusion (B_1) coefficients are defined as,

$$B_0 = \frac{1}{4}\left[\langle\langle p'^2\rangle\rangle - \frac{\langle\langle(\mathbf{p}.\mathbf{p}')^2\rangle\rangle}{p^2}\right], \tag{7}$$

$$B_1 = \frac{1}{2}\left[\frac{\langle\langle(\mathbf{p}.\mathbf{p}')^2\rangle\rangle}{p^2} - 2\langle\langle(\mathbf{p}.\mathbf{p}')\rangle\rangle + p^2\langle\langle 1\rangle\rangle\right]. \tag{8}$$

In the center-of-momentum frame of the colliding system, the thermal average of a function $F(\mathbf{p})$ for $2 \to 2$ process, in general, becomes,

$$\langle\langle F(\mathbf{p})\rangle\rangle_{col} = \frac{1}{(512\,\pi^4)E_p\gamma_{HQ}}\int_0^\infty dq\left(\frac{s-m_{HQ}^2}{s}\right)f_k(E_q) \times(1\pm f_k(E_{q'}))\int_0^\pi d\chi\,\sin\chi\int_0^\pi d\theta_{cm}\,\sin\theta_{cm} \times\sum|\mathcal{M}_{2\to2}|^2\int_0^{2\pi}d\phi_{cm}\,F(\mathbf{p}), \tag{9}$$

where χ is the angle between the heavy quark and medium particles in the lab frame and $s = (E_p + E_q)^2 - |\mathbf{p}|^2 - |\mathbf{q}|^2 - 2|\mathbf{p}||\mathbf{q}|\cos\chi$. The zenith θ_{cm} and azimuthal ϕ_{cm} angles are defined in the center-of-momentum frame. The Debye screening mass (m_D) is inserted at leading order for t-channel gluonic propagator to the in-medium matrix elements,

$$m_D^2 = (4\pi\alpha_s)\,T^2\left(\frac{N_c}{3} + \frac{N_f}{6}\right). \tag{10}$$

2.1.2 Radiative (2→3) process

Heavy quarks can also radiate soft gluons while moving through the QGP medium along with the collisions. The inelastic ($2 \to 3$) process is,

$$HQ\,(p) + lq/l\bar{q}/g\,(q) \to HQ\,(p') + lq/l\bar{q}/g(q') + g\,(k'), \tag{11}$$

where $k' \equiv (E_{k'}, \mathbf{k}'_\perp, k'_z)$ is the four-momentum of the final state soft gluon emitted by the bottom quark ($k' \to 0$). Compared to the collisional process, for the radiative process, only the kinematical and the interaction parts are modified in Eqs. (3) and (4). The general expression for the thermal averaged $F(\mathbf{p})$ for $2 \to 3$ process is [52],

$$\langle\langle F(\mathbf{p})\rangle\rangle_{rad} = \frac{1}{2E_p\gamma_{HQ}}\int\frac{d^3\mathbf{q}}{(2\pi)^3E_q}\int\frac{d^3\mathbf{q}'}{(2\pi)^3E_{q'}}\int\frac{d^3\mathbf{p}'}{(2\pi)^3E_{p'}} \times\int\frac{d^3\mathbf{k}'}{(2\pi)^3E_{k'}}\sum|\mathcal{M}_{2\to3}|^2\,\delta^{(4)}(p+q-p'-q'-k') \times(2\pi)^4\,f_k(E_q)\,(1\pm f_k(E_{q'}))\,(1+f_k(E_{k'})) \times\theta_1(E_p-E_{k'})\,\theta_2(\tau-\tau_F)\,F(\mathbf{p}), \tag{12}$$

where the theta function $\theta_1(E_p - E_{k'})$ ensures that the bottom quark initial energy E_p is always greater than radiated soft gluon energy $E_{k'}$ and $\theta_2(\tau - \tau_F)$ keep the collision time τ of the heavy quark with the medium particles always greater than the gluon formation time τ_F (Landau–Pomeranchuk–Migdal Effect) [37,47,72]. $(1+f_g(E_{k'}))$ is the Bose enhancement factor for the radiated gluon and $|\mathcal{M}_{2\to3}|^2$ is the matrix element squared for the radiative process which can be written as [4],

$$|\mathcal{M}_{2\to3}|^2 = |\mathcal{M}_{2\to2}|^2 \times\frac{12g_s^2}{(k'_\perp)^2}\left(1+\frac{m_{HQ}^2}{s}e^{2y_{k'}}\right)^{-2}, \tag{13}$$

where $y_{k'}$ is the rapidity of the emitted gluon and $\left(1+\frac{m_{HQ}^2}{s}e^{2y_{k'}}\right)^{-2}$ is the dead cone factor for the heavy

quark. The details of the soft gluon 3-momentum integral are discussed in detail in Appendix **B** of [63].

2.2 EQPM distribution of quarks and gluons in a viscous medium

EQPM include the effects of the thermal interactions of the QGP medium in the analysis via a realistic QCD equation of state. For the system close to the local equilibrium, the in-medium particle momentum distribution function has the form,

$$f_k = f_k^0 + \delta f_k \quad \text{with} \quad \delta f_k / f_k^0 \ll 1, \tag{14}$$

where f_k^0 is the EQPM equilibrium distribution function and δf_k is the non-equilibrium component. The EQPM distribution functions of light quarks/antiquarks and gluons are defined in terms of effective fugacity parameter z_k. For zero baryon chemical potential,

$$f^0_{lq/l\bar{q}} = \frac{z_{lq/l\bar{q}} \exp[-\beta(u\cdot q)]}{1 + z_{lq/l\bar{q}} \exp[-\beta(u\cdot q)]}, \tag{15}$$

$$f^0_{g} = \frac{z_{g} \exp[-\beta\,(u\cdot q)]}{1 - z_{g} \exp[-\beta\,(u\cdot q)]}. \tag{16}$$

The parameters $z_{lq/l\bar{q}}$ and z_g are effective fugacities that encode the QCD interactions for quarks/antiquarks and gluons. These temperature-dependent parameters modify the single-particle dispersion relation as,

$$\tilde{q_k}^{\mu} = q_k^{\mu} + \delta\omega_k\, u^{\mu}, \qquad \delta\omega_k = T^2\, \partial_T \ln(z_k), \tag{17}$$

where $\tilde{q}_k^{\mu} = (\omega_k, \mathbf{q}_k)$ and $q_k^{\mu} = (E_q, \mathbf{q}_k)$ are the quasiparticle (dressed) and bare particle momenta, respectively. In the limit, $z_k \to 1$, the ideal equation of state is reproduced. The effective coupling constant (α_{eff}) is introduced from the kinetic theory through EQPM-based Debye mass as [55],

$$\frac{\alpha_{eff}}{\alpha_s(T)} = \frac{\frac{2N_c}{\pi^2}\text{PolyLog}\,[3, z_g] - \frac{2N_f}{\pi^2}\text{PolyLog}\,[3, -z_{lq}]}{\left(\frac{N_c}{3} + \frac{N_f}{6}\right)}. \tag{18}$$

$\alpha_s(T)$ is the 2-loop running coupling constant at finite temperature [31,46].

The evolution of the medium particle distribution function can be described by the effective Boltzmann equation based on the EQPM and using the effective covariant kinetic theory approach. Within the relaxation time approximation (RTA), it is expressed as follows [54],

$$\tilde{q}_k^{\mu}\, \partial_{\mu} f_k(x, \tilde{q}_k) + F_k^{\mu}\, (u\cdot\tilde{q}_k)\, \partial_{\mu}^{(q)} f_k = -\,(u\cdot\tilde{q}_k)\, \frac{\delta f_k}{\tau_R}, \tag{19}$$

where τ_R is the thermal relaxation time and $F_k^{\mu} = -\partial_{\nu}(\delta\omega_k u^{\nu} u^{\mu})$ is the mean field force term. The viscous corrections to the distribution function are obtained by solving Eq. (19) using the iterative Chapman–Enskog method [43] and obtain the first order correction to the distribution function as,

$$\delta f_k = \tau_R \left(\tilde{q}_k^{\gamma}\, \partial_{\gamma}\beta + \frac{\beta\, \tilde{q}_k^{\gamma}\, \tilde{q}_k^{\phi}}{u\cdot\tilde{q}_k} \partial_{\gamma} u_{\phi} - \beta\theta\, \delta\omega_k \right) f_k^0\, \tilde{f}_k^0, \tag{20}$$

where $\tilde{f}_k{}^0 \equiv (1 - a_k f_k^0)$ ($a_g = -1$ for bosons and $a_{lq} = +1$ for fermions). The first-order evolution equation for the shear stress tensor $\pi^{\mu\nu}$ and bulk viscous pressure Π within the effective kinetic theory has the following forms [17],

$$\pi^{\mu\nu} = 2\,\tau_R\,\beta_{\pi}\,\sigma^{\mu\nu}, \qquad \Pi = -\tau_R\,\beta_{\Pi}\,\theta, \tag{21}$$

with $\theta \equiv \partial_{\mu} u^{\mu}$ as the scalar expansion parameter and $\sigma^{\mu\nu} \equiv \Delta^{\mu\nu}_{\alpha\beta}\nabla^{\alpha}u^{\beta}$ where $\Delta^{\mu\nu}_{\alpha\beta} \equiv \frac{1}{2}(\Delta^{\mu}_{\alpha}\Delta^{\nu}_{\beta} + \Delta^{\mu}_{\beta}\Delta^{\nu}_{\alpha}) - \frac{1}{3}\Delta^{\mu\nu}\Delta_{\alpha\beta}$ denotes traceless symmetric projection operator orthogonal to the fluid velocity u^{μ}. Here, β_{π} and β_{Π} are the first-order coefficients and have the form specified in [17]. Using the evolution equation, the shear and bulk viscous corrections to the distribution function can be expressed as,

$$\delta f_k = \delta f_k^{\text{shear}} + \delta f_k^{\text{bulk}}, \tag{22}$$

$$\delta f_k^{\text{shear}} = \frac{\beta\, f_k^0\, \tilde{f}_k^0}{2\beta_{\pi}(u.\tilde{q}_k)} \tilde{q}_k^{\alpha}\tilde{q}_k^{\beta}\pi_{\alpha\beta}, \tag{23}$$

$$\delta f_k^{\text{bulk}} = -\frac{\beta\, f_k^0\, \tilde{f}_k^0}{\beta_{\Pi}(u.\tilde{q}_k)} \left[(u.\tilde{q}_k)^2 c_s^2 - \frac{|\,\tilde{\mathbf{q}}_k\,|^2}{3} - (u.\tilde{q}_k)\delta\omega_k \right] \Pi. \tag{24}$$

Substituting the modified in-medium particle distribution functions with the shear and bulk viscous corrections from Eqs. (23) and (24) into Eqs. (5)–(8), we obtain the modified heavy quark drag and diffusion coefficients in the viscous medium up to the first order. Considering longitudinal boost invariant expansion through Bjorken prescription [18] and using Milne coordinates (τ, x, y, η_s), the Eqs. (23) and Eqs. (24) simplifies to,

$$\delta f_k^{\text{shear}} = \frac{f_k^0\, \tilde{f}_k^0\, \mathfrak{s}}{\beta_{\pi}\omega_k T\tau} \left(\frac{\eta}{\mathfrak{s}}\right) \left[\frac{|\mathbf{q_k}|^2}{3} - (q_k)_z^2 \right], \tag{25}$$

$$\delta f_k^{\text{bulk}} = \frac{f_k^0\, \tilde{f}_k^0\, \mathfrak{s}}{\beta_{\Pi}\omega_k T\tau} \left(\frac{\zeta}{\mathfrak{s}}\right) \left[(\omega_k)^2 c_s^2 - \frac{|\mathbf{q_k}|^2}{3} - (\omega_k)\delta\omega_k \right], \tag{26}$$

where $\tau = \sqrt{t^2 - z^2}$ is the proper time and, $\eta_s = \tanh^{-1}(z/t)$ is the space-time rapidity with $u^{\mu} = (1, 0, 0, 0)$ and $g^{\mu\nu} = (1, -1, -1, -1/\tau^2)$. Here, $\theta = 1/\tau$, $\Pi = -\zeta/\tau$ and $\pi^{\mu\nu}\sigma_{\mu\nu} = 4\eta/3\tau^2$. η and ζ denote the shear and bulk viscosity of the QGP respectively, c_s^2 is the speed of sound squared and $\mathfrak{s}$ is the entropy density of the medium.

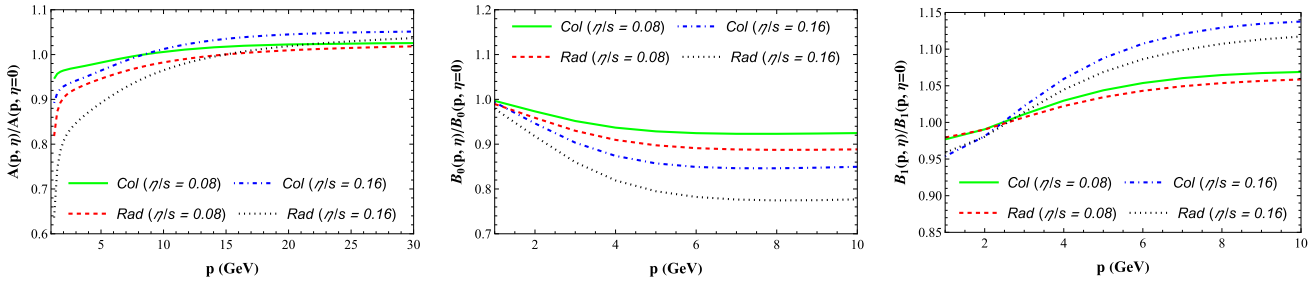

Fig. 1 Bottom quark transport coefficients with first-order shear viscous correction scaled with the corresponding value for the non-viscous case ($\eta = 0$) as a function of its initial momentum (p) at $T = 3\,T_c$

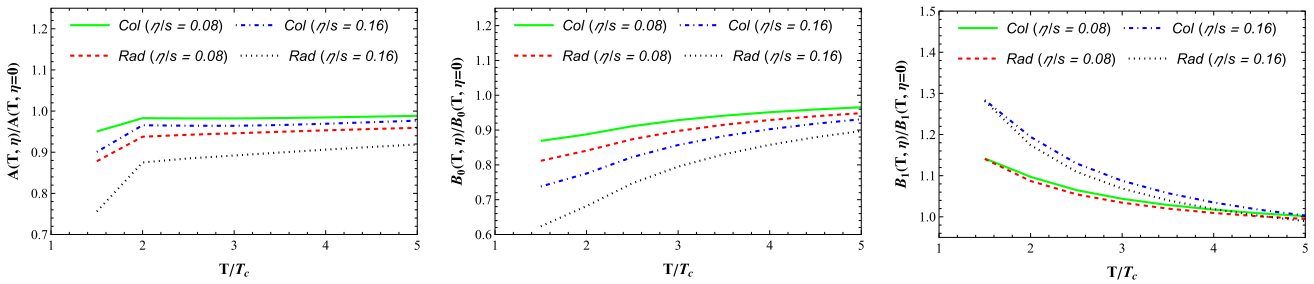

Fig. 2 Bottom quark transport coefficients with first-order shear viscous correction scaled with the corresponding value for the non-viscous case ($\eta = 0$) as a function of QGP temperature (T/T_c) for the initial momentum $p = 5$ GeV

3 Results and discussions

3.1 Bottom transport coefficients with shear viscous correction

In this study, we take the bottom quark mass $m_b = 4.2$ GeV, quark-hadron transition temperature $T_c = 170$ MeV for three massless light quark flavors with zero net baryon density and the proper time $\tau = 0.25$ fm. Figure 1 displays the effects of shear viscous correction on the momentum dependence of the bottom quark drag coefficient for collisional and radiative processes in the QGP. The transport coefficients are scaled with their respective values for the $\eta = 0$ case. The momentum and temperature dependence of the transport coefficients due to the collisional and radiative processes can be described using Eqs. (5–9, 12). It is observed that the shear viscosity substantially reduces the heavy quark drag ($A(\eta)/A(\eta = 0)$) (left panel) at low momenta ($p \approx 1 - 8$ GeV for collision and $p \approx 1 - 14$ GeV for radiation). However, in the high momentum regime ($p \gtrsim 15$ GeV), the drag coefficient increases with an increase in the shear viscosity to entropy density ratio $\eta/\mathfrak{s}$. This can be understood from the interplay of two terms in Eq. (5) in different momentum regimes while incorporating the viscous effects through Eq. (25). The shear viscous correction is more prominent for the low momenta of the bottom quark – with an increase in the shear viscosity resulting in a decrease in the drag coefficient for both collisional and radiative processes. The radiative curves for low initial momentum are affected more as compared to the collisional ones whereas if we look towards the higher momenta ($p \approx 30$ GeV) the radiative curves show less sensitivity to the change in $\eta/\mathfrak{s}$. This is because the radiative process is suppressed for the bottom quark due to the dead-cone effect for gluon emission angles smaller than $\theta_k \sim m_{HQ}/E_{HQ}$. In the Fig. 1 (middle panel), the scaled transverse diffusion coefficient $B_0(\eta)/B_0(\eta = 0)$ deviate slightly from the ideal case ($\eta = 0$) near low momentum with considerable suppression towards higher momentum values. Further, the increase in shear viscosity leads to more deviation from the equilibrium with the radiative curves being more suppressed than the collisional ones for a given $\eta/\mathfrak{s}$. The longitudinal diffusion coefficient ($B_1(\eta)/B_1(\eta = 0)$) (right panel) is reduced due to shear viscous correction at low momenta ($p \lesssim 2$ GeV) affecting both collisional and radiative curves nearly the same with the variation of $\eta/\mathfrak{s}$. For momenta $p \gtrsim 4$ GeV, the behaviour is observed to be quite the opposite to that for low momenta where the longitudinal diffusion coefficient increase compared to its value in the absence of shear viscosity and higher $\eta/\mathfrak{s}$ showing a larger deviation.

Figure 2 shows the effect of variation of the scaled transport coefficients of the bottom quark as a function of the scaled QGP temperature (T/T_c). Introducing the shear viscous correction considerably reduces the bottom quark drag coefficient near T_c. This behaviour can be explained by the negative contribution from the factor $\left[\frac{|\mathbf{q_k}|^2}{3} - (q_k)_z^2\right]$ in Eq. (25) for δf_k^{shear}. The shear viscosity effect is more pronounced near the transition temperature due to the temper-

ature dependence of β_π ($\beta_\pi \propto T^4$) such that $\frac{\mathfrak{s}}{\beta_\pi T} \propto \frac{1}{T^2}$ in Eq. (25). Qualitatively similar behaviour is observed for the temperature dependence of the transverse diffusion coefficient $B_0(\eta)/B_0(\eta = 0)$ (middle panel) of the bottom quark with relatively large suppression of the ratio near $1.5T_c$. There is also an overall suppression observed with increasing $\eta/\mathfrak{s}$ for both collisional and radiative curves, with the latter being affected more over the entire temperature range considered here. Contrary to the drag and transverse diffusion coefficients, the bottom quark longitudinal diffusion coefficient $B_1(\eta)/B_1(\eta = 0)$ (right panel) seems to increase with an increase in $\eta/\mathfrak{s}$ for both collisional and radiative processes for $T < 4\,T_c$. Following the same argument as before for the drag coefficient, the effect of shear viscous correction (entering through Eq. (25) with $\frac{\mathfrak{s}}{\beta_\pi T} \propto \frac{1}{T^2}$) to the diffusion coefficients is more visible for low temperatures.

The fluctuation–dissipation theorem (FDT) gives the relation between the drag and diffusion coefficients of heavy quarks. In our study, where non-equilibrated degrees of freedom (heavy quarks) evolve in the background of an equilibrated plasma, we check the validity of this theorem in the momentum regime considered in our study. In the non-relativistic limit, $B/A = E\,T$, where E is the energy of the heavy quark and T is the temperature. This relation ensures that in the long-time limit, the phase-space distribution function aptly describes the equilibration of the heavy quark with the medium [38,68]. For small momentum, both transverse and longitudinal momentum diffusion coefficients become approximately equal, $B_0 = B_1 \equiv B$. Additionally, in this study, we have combined the collisional and radiative processes. Note that for low momentum, this sum is dominated by the contribution from the collisional process. From Fig. 3, we observe that without the shear viscous correction ($\eta/\mathfrak{s} = 0$), within EQPM, the FDT is almost satisfied for low momentum ($3\,\text{GeV} \lesssim p \lesssim 6\,\text{GeV}$) and is violated for high momentum. As we include the non-equilibrium (shear viscosity) corrections to the transport coefficients, the FDT is not valid for $\eta/\mathfrak{s} = 0.08, 0.16$, even for low momentum. Recently, the effect of initial state fluctuations on the heavy quark transport coefficients is studied in the viscous hydrodynamic model and its role in the experimental observables (R_{AA} and v_2) of open charm mesons in heavy-ion collision experiments [65].

3.2 Bottom transport coefficients with bulk viscous correction

In Fig. 4 (left panel), the effect of bulk viscous correction on the momentum dependence of the bottom quark drag coefficient ($A(\zeta)/A(\zeta = 0)$) is shown. The bulk viscosity reduce the heavy quark drag with almost constant dependence throughout the momentum range considered here. For both collisional and radiative energy loss, the drag coefficient ratio decreases with an increase in the bulk viscosity to entropy density ratio ($\zeta/\mathfrak{s}$). This can be understood by the suppression of δf_k^{bulk} due to the negative terms in Eq. (26) with an increase in $\zeta/\mathfrak{s}$. Figure 4 (right panel) shows the effect of the variation of the scaled drag coefficient as a function of the scaled QGP temperature T/T_c. The bulk viscosity effect is prominent near the transition temperature $T \approx 1.5\,T_c$ and the drag coefficient approaches the conformal limit ($c_s^2 \approx \frac{1}{3}$) at high temperatures $T \gtrsim 4\,T_c$. This behaviour can be explained from Eq. (26) wherein for $T >> T_c$, we have $z_k \to 1$ (ideal equation of state) and the medium modified part of the dispersion relation vanishes, *i.e.*, $\delta\omega_k \to 0$ in Eq. (17). The first and second terms in Eq. (26) cancel each other for the case of massless quasiparticles, leading to effectively zero contribution from δf_k^{bulk} at high temperatures. We also notice that both collisional and radiative processes show identical behaviour with the variation in bulk viscosity; consistent with our previous study for the charm quark [62]. The transverse and longitudinal diffusion coefficients plots including the bulk viscous corrections show similar trends as for the drag coefficient shown in fig. 4.

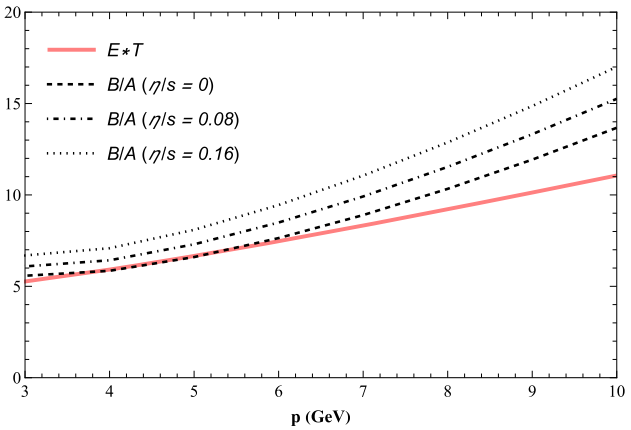

Fig. 3 Ratio of diffusion to drag (B/A) for the bottom quark with first-order shear viscous correction as a function of its initial momentum (p) at $T = 3\,T_c = 510$ MeV. A solid line indicates the product of bottom quark energy (E) and medium temperature (T)

3.3 Collisional and radiative energy loss of charm and bottom quarks

The drag coefficient gives the measure of the resistance to the motion of the heavy quark due to the thermal QGP constituents. The differential energy loss of the heavy quark is related to its drag coefficient as [34],

$$-\frac{dE}{dx} = p\,A(p). \tag{27}$$

Fig. 5 (left panel) shows the ratio ($\mathcal{R}$) of the differential energy loss for the radiative (inelastic) process to the collisional (elastic) energy loss for charm ($m_c = 1.3$ GeV)

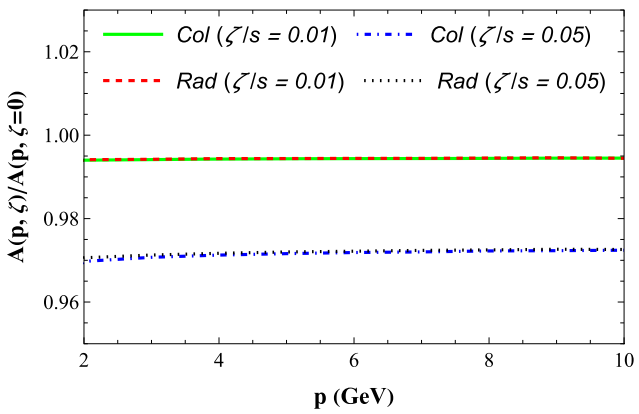

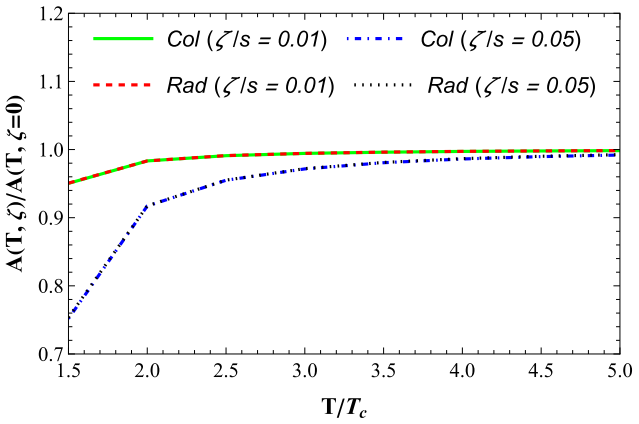

Fig. 4 Bottom quark drag coefficient with first-order bulk viscous correction and scaled with the corresponding value for the non-viscous case ($\zeta = 0$) as a function of its initial momentum (p) at $T = 3\,T_c$ (left panel), and as a function of scaled QGP temperature (T/T_c) at $p = 5$ GeV (right panel)

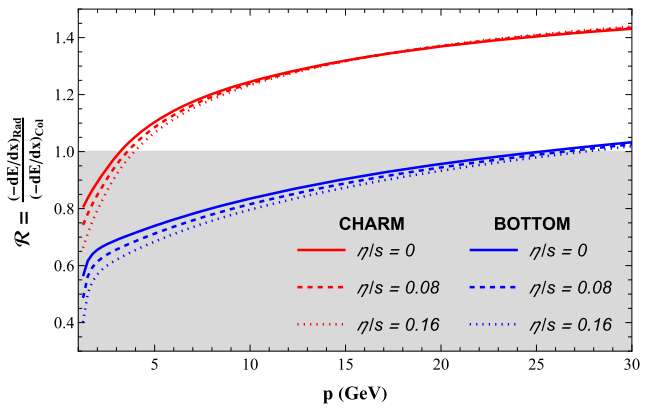

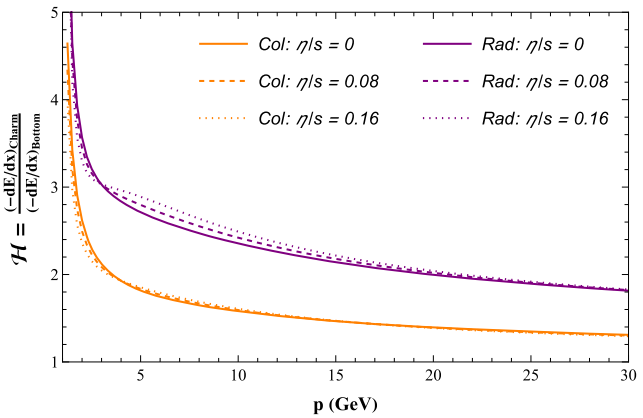

Fig. 5 (Left panel) Ratio of the radiative to collisional differential energy loss for the charm quark (red curves) and the bottom quark (blue curves) at $3\,T_c$. (Right panel) Ratio of charm to bottom quarks energy loss due to collision (orange curves) and radiation (purple curves) at $3\,T_c$

and bottom ($m_b = 4.2$ GeV) at different values of shear viscosity to entropy density ratio ($\eta/\mathfrak{s}$). For both the heavy quarks, increasing shear viscosity decreases the radiative to collisional energy loss ratio, especially near low momentum ($p \sim m_{HQ}$). However, the viscous corrections have a negligible effect at high momentum ($p >> m_{HQ}$). The suppression in the radiative energy loss of the bottom quark is significantly more compared to the charm quark. The radiative dominance for the bottom quark occurs at around 30 GeV which is almost ten times larger than that for the charm quark where the ratio exceeds one at around 3 GeV. This behaviour can be attributed to the dead-cone effect which suppresses the soft-gluon radiation by a heavy quark at angles smaller than $\theta_k \sim m_{HQ}/E_{HQ}$. The bottom quark is roughly three times more massive compared to the charm quark. Hence, its dead cone angle, where there is the absence of gluon radiation, is larger and the probability of energy loss due to radiation is lesser compared to the charm. Also, notice that the slope of the ratio where the radiative dominance occurs is larger for charm compared to the bottom. This suggest that the transition from collisional to radiative dominance of energy loss is rather more sensitive for charm with respect to the change in its initial momentum.

Figure 5 (right panel) shows the ratio ($\mathcal{H}$) of the differential energy loss for the charm quark ($m_c = 1.3$ GeV) to the bottom quark ($m_b = 4.2$ GeV) for collision and radiative processes at different values of specific shear viscosity ($\eta/\mathfrak{s}$). This ratio is equivalent to the ratio of the drag coefficients of the two heavy quarks as evident from Eq. (27). Two interesting features can be observed in this plot. First, this ratio ($\mathcal{H}$) is greater for the radiative process implying that the charm quark suffers more energy loss due to radiation than the bottom quark. Also, the ratio for the collisional case is more closer to $\mathcal{H} = 1$ compared to radiation, implying the

difference in energy loss between charm and bottom owing to their dissimilar mass, can be attributed significantly to the soft gluon radiation. Secondly, the effect of the change in $\eta/\mathfrak{s}$ over the range 0–0.16 seems to be prominent for the radiative process for initial momentum between 2 to 15 GeV compared to collision. This suggests that the medium-induced bremsstrahlung of heavy quarks is affected more due to the dissipative effects generated through shear viscosity of the medium and it is larger for the charm quark in comparison to the bottom.

4 Conclusion

The bottom quark transport coefficients have been investigated in the viscous QGP by considering its Brownian motion in the medium using the Fokker–Planck dynamics. The energy loss in the inelastic process of soft gluon radiation by the bottom quark is studied along with the elastic collision with the medium constituents. The thermal medium interactions are included through EQPM in the analysis through the temperature-dependent effective fugacity parameter for the in-medium particles. The shear and bulk viscous corrections at leading order are incorporated into the quarks, antiquarks, and gluon momentum distribution functions which are obtained by solving the effective Boltzmann equation within the EQPM framework.

The shear and bulk viscous corrections to the bottom quark drag and momentum diffusion coefficients have been estimated as a function of its initial momentum and the QGP temperature. We observe that the shear viscous correction to the bottom quark transport coefficients is prominent at the low initial momentum of the bottom quark and near the transition temperature T_c. Similar results for the charm quark have been observed in an earlier study [63]. The radiative curves seem to be affected slightly more due to a change in $\eta/\mathfrak{s}$ compared to the collision case. Furthermore, we find that the fluctuation–dissipation theorem holds valid for the bottom quark within the EQPM framework for low momentum and in the absence of shear viscous correction.

Results obtained by including the first-order bulk viscous correction are also presented here for the bottom quark drag coefficient. At $3\,T_c$, the bulk viscous correction tends to decrease the heavy quark transport coefficients consistently throughout the entire momentum regime considered here with further suppression due to increasing $\zeta/\mathfrak{s}$. The temperature dependence of the bottom transport coefficient for initial momentum of $p = 5$ GeV due to bulk viscous correction shows a considerable modification of the transport coefficient ratio near T_c which at the high temperature approaches the conformal limit ($\epsilon = 3P$). The effect of including bulk viscous correction is almost identical for the collisional and radiative processes, suggesting its minimal effect on the two processes as compared to the shear viscous correction.

The differential energy loss ratios for the radiative to collisional process and the charm to bottom quark energy loss have been investigated and comparatively studied. We conclude that radiation is the dominant process of energy loss for charm quark with momentum $p \gtrsim 4$ GeV. However, for the bottom quark, the radiative energy loss becomes significant at a much higher value of its initial momentum, indicating the importance of considering the radiative process for momenta $p \gtrsim 30$ GeV.

Acknowledgements The authors acknowledge Santosh Kumar Das for reading and providing useful comments on the manuscript. S.D. would like to acknowledge the SERB Power Fellowship, SPF/2022/000014 for the support on this work.

Data Availability Statement This manuscript has no associated data or the data will not be deposited. [Authors' comment: There is no data to be deposited.]

Funded by SCOAP^3. SCOAP^3 supports the goals of the International Year of Basic Sciences for Sustainable Development.

A Appendix: Thermodynamic integrals

The thermodynamic integrals $\tilde{J}^{(r)}_{k\,nm}$ and $\tilde{L}^{(r)}_{k\,nm}$ are respectively defined as follows,

$$\tilde{J}^{(r)}_{k\,nm} = \frac{\gamma_k}{2\pi^2}\frac{(-1)^m}{(2m+1)!!}\int_0^\infty d\mid\tilde{\mathbf{p}}_k\mid\left(u\cdot\tilde{p}_k\right)^{n-2m-r-1} \times\left(\mid\tilde{\mathbf{p}}_k\mid\right)^{2m+2} f^0_k\,\tilde{f}^0_k, \tag{28}$$

$$\tilde{L}^{(r)}_{k\,nm} = \frac{\gamma_k}{2\pi^2}\frac{(-1)^m}{(2m+1)!!}\int_0^\infty d\mid\tilde{\mathbf{p}}_k\mid\frac{\left(u.\tilde{p}_k\right)^{n-2m-r-1}}{\mid\tilde{\mathbf{p}}_k\mid} \times\left(\mid\tilde{\mathbf{p}}_k\mid\right)^{2m+2} f^0_k\,\tilde{f}^0_k. \tag{29}$$

For the massless limit of the light quark, the thermodynamic integrals can be expressed in terms of the $PolyLog$ function as follows,

$$\tilde{J}^{(1)}_{k\ 42} = -\frac{2\,a_k\gamma_k T^5}{5\pi^2}\Bigg[2\,\text{PolyLog}\,[4,-a_k z_k] - \frac{\delta\omega_k}{T}\,\text{PolyLog}\,[3,-a_k z_k]\Bigg], \tag{30}$$

$$\tilde{L}^{(1)}_{k\ 42} = -\frac{a_k\gamma_k T^4}{5\pi^2}\,\text{PolyLog}\,[3,-a_k z_k]. \tag{31}$$

References

1. K. Aamodt et al., Charged-particle multiplicity density at mid-rapidity in central Pb–Pb collisions at $\sqrt{s_{NN}} = 2.76$ TeV. Phys. Rev. Lett. **105**, 252301 (2010). https://doi.org/10.1103/PhysRevLett.105.252301. arXiv:1011.3916 [nucl-ex]
2. G. Aarts et al., Heavy-flavor production and medium properties in high-energy nuclear collisions – what next?'. Eur. Phys. J. A **53**(5), 93 (2017). https://doi.org/10.1140/epja/i2017-12282-9. arXiv:1612.08032 [nucl-th]
3. R. Abir et al., Heavy quark energy loss and Dmesons in RHIC and LHC energies. Phys. Lett. B **715**, 183–189 (2012). https://doi.org/10.1016/j.physletb.2012.07.044. arXiv:1203.5221 [hep-ph]
4. R. Abir et al., Soft gluon emission off a heavy quark revisited. Phys. Rev. D **85**, 054012 (2012). https://doi.org/10.1103/PhysRevD.85.054012. arXiv:1109.5539 [hep-ph]
5. S. Acharya et al., Prompt D0, D+, and D.+ production in Pb.Pb collisions at $\sqrt{s_{NN}} = 5.02$ TeV. JHEP **01**, 174 (2022). https://doi.org/10.1007/JHEP01(2022)174. arXiv:2110.09420 [nucl-ex]
6. J. Adams et al., Experimental and theoretical challenges in the search for the quark gluon plasma: the STAR Collaboration's critical assessment of the evidence from RHIC collisions. Nucl. Phys. A **757**, 102–183 (2005). https://doi.org/10.1016/j.nuclphysa.2005.03.085. arXiv:nucl-ex/0501009
7. A. Adare et al., Energy loss and flow of heavy quarks in Au+Au collisions at s(NN)**(1/2) = 200-GeV. Phys. Rev. Lett. **98**, 172301 (2007). https://doi.org/10.1103/PhysRevLett.98.172301. arXiv:nucl-ex/0611018
8. K. Adcox et al., Formation of dense partonic matter in relativistic nucleus-nucleus collisions at RHIC: experimental evaluation by the PHENIX collaboration. Nucl. Phys. A **757**, 184–283 (2005). https://doi.org/10.1016/j.nuclphysa.2005.03.086. arXiv:nucl-ex/0410003
9. S.S. Adler et al., Nuclear modification of electron spectra and implications for heavy quark energy loss in Au+Au collisions at s(NN)**(1/2) - 200-GeV. Phys. Rev. Lett. **96**, 032301 (2006). https://doi.org/10.1103/PhysRevLett.96.032301. arXiv:nucl-ex/0510047
10. Y. Akamatsu, T. Hatsuda, T. Hirano, Heavy quark diffusion with relativistic Langevin dynamics in the quark–gluon fluid. Phys. Rev. C **79**, 054907 (2009). https://doi.org/10.1103/PhysRevC.79.054907. arXiv:0809.1499 [hep-ph]
11. W.M. Alberico et al., Heavy flavors in AA collisions: production, transport and final spectra. Eur. Phys. J. C **73**, 2481 (2013). https://doi.org/10.1140/epjc/s10052-013-2481-z. arXiv:1305.7421 [hep-ph]
12. A. Andronic et al., Heavy-flavour and quarkonium production in the LHC era: from proton–proton to heavy-ion collisions. Eur. Phys. J. C **76**(3), 107 (2016). https://doi.org/10.1140/epjc/s10052-015-3819-5. arXiv:1506.03981 [nucl-ex]
13. I. Arsene et al., Quark gluon plasma and color glass condensate at RHIC? The perspective from the BRAHMS experiment. Nucl. Phys. A **757**, 1–27 (2005). https://doi.org/10.1016/j.nuclphysa.2005.02.130. arXiv:nucl-ex/0410020
14. B.B. Back et al., The PHOBOS perspective on discoveries at RHIC. Nucl. Phys. A **757**, 28–101 (2005). https://doi.org/10.1016/j.nuclphysa.2005.03.084. arXiv:nucl-ex/0410022
15. D. Banerjee et al., Heavy quark momentum diffusion coefficient from lattice QCD. Phys. Rev. D **85**, 014510 (2012). https://doi.org/10.1103/PhysRevD.85.014510. arXiv:1109.5738 [hep-lat]
16. A. Beraudo et al., Extraction of heavy-flavor transport coefficients in QCD matter. Nucl. Phys. A **979**, 21–86 (2018). https://doi.org/10.1016/j.nuclphysa.2018.09.002. arXiv:1803.03824 [nucl-th]
17. S. Bhadury et al., First order dissipative hydrodynamics and viscous corrections to the entropy four-current from an effective covariant kinetic theory. J. Phys. G **47**(8), 085108 (2020). https://doi.org/10.1088/1361-6471/ab907b. arXiv:1902.05285 [hep-ph]
18. J.D. Bjorken, Highly relativistic nucleus–nucleus collisions: the Central Rapidity Region. Phys. Rev. D **27**, 140–151 (1983). https://doi.org/10.1103/PhysRevD.27.140
19. E. Braaten, M.H. Thoma, Energy loss of a heavy quark in the quark–gluon plasma. Phys. Rev. D **44**(9), 2625 (1991). https://doi.org/10.1103/PhysRevD.44.R2625
20. N. Brambilla et al., Lattice QCD constraints on the heavy quark diffusion coefficient. Phys. Rev. D **102**(7), 074503 (2020). https://doi.org/10.1103/PhysRevD.10. arXiv:2007.10078 [hep-lat]
21. S. Cao et al., Toward the determination of heavy-quark transport coefficients in quark–gluon plasma. Phys. Rev. C **99**(5), 054907 (2019). https://doi.org/10.1103/PhysRevC.99.054907. arXiv:1809.07894 [nucl-th]
22. S. Cao, G.-Y. Qin, S.A. Bass, Energy loss, hadronization and hadronic interactions of heavy flavors in relativistic heavy-ion collisions. Phys. Rev. C **92**(2), 024907 (2015). https://doi.org/10.1103/PhysRevC.92.024907. arXiv:1505.01413 [nucl-th]
23. S. Cao, G.-Y. Qin, S.A. Bass, Heavy-quark dynamics and hadronization in ultrarelativistic heavy-ion collisions: collisional versus radiative energy loss. Phys. Rev. C **88**, 044907 (2013). https://doi.org/10.1103/PhysRevC.88.044907. arXiv:1308.0617 [nucl-th]
24. S. Cao et al., Linearized Boltzmann transport model for jet propagation in the quark-gluon plasma: heavy quark evolution. Phys. Rev. C **94**(1), 014909 (2016). https://doi.org/10.1103/PhysRevC.94.014909. arXiv:1605.06447 [nucl-th]
25. V. Chandra, V. Ravishankar, A quasi-particle description of (2+1)-flavor lattice QCD equation of state. Phys. Rev. D **84**, 074013 (2011). https://doi.org/10.1103/PhysRevD.84.074013. arXiv:1103.0091 [nucl-th]
26. V. Chandra, V. Ravishankar, Quasi-particle model for lattice QCD: quark–gluon plasma in heavy ion collisions. Eur. Phys. J. C **64**, 63–72 (2009). https://doi.org/10.1140/epjc/s10052-009-1126-8. arXiv:0812.1430 [nucl-th]
27. S.K. Das, J. Alam, P. Mohanty, Dragging heavy quarks in quark gluon plasma at the large hadron collider. Phys. Rev. C **82**, 014908 (2010). https://doi.org/10.1103/PhysRevC.82.014908. arXiv:1003.5508 [nucl-th]
28. S.K. Das, J. Alam, P. Mohanty, Probing quark gluon plasma properties by heavy flavours. Phys. Rev. C **80**, 054916 (2009). https://doi.org/10.1103/PhysRevC.80.054916. arXiv:0908.4194 [nucl-th]
29. S.K. Das, V. Chandra, J. Alam, Heavy-quark transport coefficients in a hot viscous quark–gluon plasma medium. J. Phys. G **41**, 015102 (2013). https://doi.org/10.1088/0954-3899/41/1/015102. arXiv:1210.3905 [nucl-th]
30. S.K. Das et al., Heavy-flavor in-medium momentum evolution: Langevin versus Boltzmann approach. Phys. Rev. C **90**, 044901 (2014). https://doi.org/10.1103/PhysRevC.90.044901. arXiv:1312.6857 [nucl-th]
31. S.K. Das et al., Toward a solution to the RAA and v2 puzzle for heavy quarks. Phys. Lett. B **747**, 260–264 (2015). https://doi.org/10.1016/j.physletb.2015.06.003. arXiv:1502.03757 [nucl-th]

32. X. Dong, V. Greco, Heavy quark production and properties of quark–gluon plasma. Prog. Part. Nucl. Phys. **104**, 97–141 (2019). https://doi.org/10.1016/j.ppnp.2018.08.001
33. C. Gale, S. Jeon, B. Schenke, Hydrodynamic modeling of heavy-ion collisions. Int. J. Mod. Phys. A **28**, 1340011 (2013). https://doi.org/10.1142/S0217751X13400113. arXiv:1301.5893 [nucl-th]
34. M. Golam Mustafa, D. Pal, D.K. Srivastava, Propagation of charm quarks in equilibrating quark–gluon plasma. Phys. Rev. C **57**, 889–898 (1998). https://doi.org/10.1103/PhysRevC.57.3499. arXiv:nucl-th/9706001. [Erratum: Phys. Rev. C 57, 3499-3499 (1998)]
35. P.B. Gossiaux, J. Aichelin, Towards an understanding of the RHIC single electron data. Phys. Rev. C **78**, 014904 (2008). https://doi.org/10.1103/PhysRevC.78.014904. arXiv:0802.2525 [hep-ph]
36. P.B. Gossiaux, V. Guiho, J. Aichelin, Heavy quarks thermalization in heavy-ion ultrarelativistic collisions: elastic or radiative? J. Phys. G **32**, S359–S364 (2006). https://doi.org/10.1088/0954-3899/32/12/S44
37. M. Gyulassy, X. Wang, Multiple collisions and induced gluon Bremsstrahlung in QCD. Nucl. Phys. B **420**, 583–614 (1994). https://doi.org/10.1016/0550-3213(94)90079-5. arXiv:nucl-th/9306003
38. M. He, H. van Hees, R. Rapp, Heavy-quark diffusion in the quark–gluon plasma. (2022). arXiv:2204.09299 [hep-ph]
39. H. van Hees et al., Nonperturbative heavy-quark diffusion in the quark–gluon plasma. Phys. Rev. Lett. **100**, 192301 (2008). https://doi.org/10.1103/PhysRevLett.100.192301. arXiv:0709.2884 [hep-ph]
40. H. van Hees, V. Greco, R. Rapp, Heavy-quark probes of the quark–gluon plasma at RHIC. Phys. Rev. C **73**, 034913 (2006). https://doi.org/10.1103/PhysRevC.73.034913. arXiv:nucl-th/0508055
41. U. Heinz, R. Snellings, Collective flow and viscosity in relativistic heavy-ion collisions. Ann. Rev. Nucl. Part. Sci. **63**, 123–151 (2013). https://doi.org/10.1146/annurev-nucl-102212-170540. arXiv:1301.2826 [nucl-th]
42. A. Jaiswal et al., Dynamics of QCD matter – current status. Int. J. Mod. Phys. E **30**(02), 2130001 (2021). https://doi.org/10.1142/S0218301321300010. arXiv:2007.14959 [hep-ph]
43. A. Jaiswal, Relativistic dissipative hydrodynamics from kinetic theory with relaxation time approximation. Phys. Rev. C **87**(5), 051901 (2013). https://doi.org/10.1103/PhysRevC.87.051901. arXiv:1302.6311 [nucl-th]
44. A. Jaiswal, V. Roy, Relativistic hydrodynamics in heavy-ion collisions: general aspects and recent developments. Adv. High Energy Phys. **2016**, 9623034 (2016). https://doi.org/10.1155/2016/9623034. arXiv:1605.08694 [nucl-th]
45. M.Y. Jamal, B. Mohanty, Passage of heavy quarks through the fluctuating hot QCD medium. (2021). arXiv:2101.00164 [nucl-th]
46. O. Kaczmarek, F. Zantow, Static quark anti-quark interactions in zero and finite temperature QCD. I. Heavy quark free energies, running coupling and quarkonium binding. Phys. Rev. D **71**, 114510 (2005). https://doi.org/10.1103/PhysRevD.71.114510. arXiv:hep-lat/0503017
47. S. Klein, Suppression of Bremsstrahlung and pair production due to environmental factors. Rev. Mod. Phys. **71**, 1501–1538 (1999). https://doi.org/10.1103/RevModPhys.71.1501. arXiv:hep-ph/9802442
48. M. Kurian, V. Chandra, S.K. Das, Impact of longitudinal bulk viscous effects to heavy quark transport in a strongly magnetized hot QCD medium. Phys. Rev. D **101**(9), 094024 (2020). https://doi.org/10.1103/PhysRevD.101.094024. arXiv:2002.03325 [nucl-th]
49. M. Kurian et al., Charm quark dynamics in quarkgluon plasma with 3 + 1D viscous hydrodynamics. Phys. Rev. C **102**(4), 044907 (2020). https://doi.org/10.1103/PhysRevC.102.044907. arXiv:2007.07705 [hep-ph]
50. S. Li et al., Probing the transport properties of quark–gluon plasma via heavy-flavor Boltzmann and Langevin dynamics. Phys. Rev. C **99**(5), 054909 (2019). https://doi.org/10.1103/PhysRevC.99.054909. arXiv:1901.04600 [hep-ph]
51. S.Y.F. Liu, R. Rapp, Nonperturbative effects on radiative energy loss of heavy quarks. JHEP **08**, 168 (2020). https://doi.org/10.1007/JHEP08(2020)168. arXiv:2003.12536 [nucl-th]
52. S. Mazumder, T. Bhattacharyya, J. Alam, Gluon bremsstrahlung by heavy quarks – its effects on transport coefficients and equilibrium distribution. Phys. Rev. D **89**(1), 014002 (2014). https://doi.org/10.1103/PhysRevD.89.014002. arXiv:1305.6445 [nucl-th]
53. S. Mazumder et al., Momentum dependence of drag coefficients and heavy flavour suppression in quark gluon plasma. Phys. Rev. C **84**, 044901 (2011). https://doi.org/10.1103/PhysRevC.84.044901. arXiv:1106.2615 [nucl-th]
54. S. Mitra, V. Chandra, Covariant kinetic theory for effective fugacity quasiparticle model and first order transport coefficients for hot QCD matter. Phys. Rev. D **97**(3), 034032 (2018). https://doi.org/10.1103/PhysRevD.97.034032. arXiv:1801.01700 [nucl-th]
55. S. Mitra, V. Chandra, Transport coefficients of a hot QCD medium and their relative significance in heavy-ion collisions. Phys. Rev. D **96**(9), 094003 (2017). https://doi.org/10.1103/PhysRevD.96.094003. arXiv:1702.05728 [nucl-th]
56. M.G. Mustafa, Energy loss of charm quarks in the quark–gluon plasma: collisional versus radiative. Phys. Rev. C **72**, 014905 (2005). https://doi.org/10.1103/PhysRevC.72.014905. arXiv:hep-ph/0412402
57. F. Prino, R. Rapp, Open heavy flavor in QCD matter and in nuclear collisions. J. Phys. G **43**(9), 093002 (2016). https://doi.org/10.1088/0954-3899/43/9/093002. arXiv:1603.00529 [nucl-ex]
58. P. Romatschke, U. Romatschke, Viscosity information from relativistic nuclear collisions: how perfect is the fluid observed at RHIC? Phys. Rev. Lett. **99**, 172301 (2007). https://doi.org/10.1103/PhysRevLett.99.172301. arXiv:0706.1522 [nucl-th]
59. S. Ryu et al., Importance of the bulk viscosity of QCD in ultrarelativistic heavy-ion collisions. Phys. Rev. Lett. **115**(13), 132301 (2015). https://doi.org/10.1103/PhysRevLett.115.132301. arXiv:1502.01675 [nucl-th]
60. S. Sarkar, C. Chattopadhyay, S. Pal, Radiative heavy quark energy loss in an expanding viscous QCD plasma. Phys. Rev. C **97**(6), 064916 (2018). https://doi.org/10.1103/PhysRevC.97.064916. arXiv:1801.00637 [nucl-th]
61. F. Scardina et al., Estimating the charm quark diffusion coefficient and thermalization time from D meson spectra at energies available at the BNL relativistic heavy ion collider and the CERN large hadron collider. Phys. Rev. C **96**(4), 044905 (2017). https://doi.org/10.1103/PhysRevC.96.044905. arXiv:1707.05452 [nucl-th]
62. A. Shaikh et al., Charm quark transport within viscous QCD medium: colliding and radiating. In: PoS CHARM2020, p. 060 (2021). https://doi.org/10.22323/1.385.0060
63. A. Shaikh et al., Heavy quark transport coefficients in a viscous QCD medium with collisional and radiative processes. Phys. Rev. D **104**(3), 034017 (2021). https://doi.org/10.1103/PhysRevD.104.034017. arXiv:2105.14296 [hep-ph]
64. B. Singh, H. Mishra, Heavy quark transport in a viscous semi QGP. Phys. Rev. D **101**(5), 054027 (2020). https://doi.org/10.1103/PhysRevD.101.054027. arXiv:1911.06764 [hep-ph]
65. M. Singh et al., Open charm phenomenology with a multistage approach to relativistic heavyion collisions. (2023). arXiv:2306.09514 [nucl-th]
66. T. Song et al., Exploring non-equilibrium quarkgluon plasma effects on charm transport coefficients. Phys. Rev. C **101**(4), 044901 (2020). https://doi.org/10.1103/PhysRevC.101.044901. arXiv:1910.09889 [nucl-th]

67. T. Song et al., Tomography of the quark–gluon–plasma by charm quarks. Phys. Rev. C **92**(1), 014910 (2015). https://doi.org/10.1103/PhysRevC.92.014910. arXiv:1503.03039 [nucl-th]
68. P.K. Srivastava, B.K. Patra, Drag and diffusion of heavy quarks in a hot and anisotropic QCD medium. Eur. Phys. J. A **53**(6), 116 (2017). https://doi.org/10.1140/epja/i2017-12299-0. arXiv:1601.02341 [hep-ph]
69. B. Svetitsky, Diffusion of charmed quarks in the quark–gluon plasma. Phys. Rev. D **37**, 2484–2491 (1988). https://doi.org/10.1103/PhysRevD.37.2484
70. J. Uphoff et al., Elastic and radiative heavy quark interactions in ultra-relativistic heavy-ion collisions. J. Phys. G **42**(11), 115106 (2015). https://doi.org/10.1088/0954-3899/42/11/115106. arXiv:1408.2964 [hep-ph]
71. J. Uphoff et al., Elliptic flow and energy loss of heavy quarks in ultra-relativistic heavy ion collisions. Phys. Rev. C **84**, 024908 (2011). https://doi.org/10.1103/PhysRevC.84.024908. arXiv:1104.2295 [hep-ph]
72. X.-N. Wang, M. Gyulassy, M. Plumer, The LPM effect in QCD and radiative energy loss in a quark gluon plasma. Phys. Rev. D **51**, 3436–3446 (1995). https://doi.org/10.1103/PhysRevD.51.3436. arXiv:hep-ph/9408344
73. H. Xu et al., Charm quarks in medium and their contribution to di-electron spectra in relativistic heavy ion collisions. Phys. Rev. C **89**, 024905 (2014). https://doi.org/10.1103/PhysRevC.89.024905. arXiv:1305.7302 [nucl-th]
74. X. Yingru et al., Resolving discrepancies in the estimation of heavy quark transport coefficients in relativistic heavy-ion collisions. Phys. Rev. C **99**(1), 014902 (2019). https://doi.org/10.1103/PhysRevC.99.014902. arXiv:1809.10734 [nucl-th]
75. D. Zigic et al., DREENA-B framework: first predictions of RAA and v2 within dynamical energy loss formalism in evolving QCD medium. Phys. Lett. B **791**, 236–241 (2019). https://doi.org/10.1016/j.physletb.2019.02.020. arXiv:1805.04786 [nucl-th]